ELSEVIER

Journal of Photochemistry and Photobiology A: Chemistry 93 (1996) 83–87

Journal of PHOTOCHEMISTRY AND PHOTOBIOLOGY A:CHEMISTRY

Quantum yields of CO_2 and SO_2 formation from 193 nm photo-oxidation of CO in a sulfuric acid aerosol

Clinton T. Mills, Glenn A. Rowland, Jan Westergren, Leon F. Phillips

Chemistry Department, University of Canterbury, Christchurch 1, New Zealand

Received 19 May 1995; accepted 11 July 1995

Abstract

The measured quantum yield of CO_2 is 1.2% for acid strengths in the range 80–100 wt.% under conditions in which the yield varies linearly with the average laser power and is independent of the CO flow. The yield of SO_2 is highly variable and may be either positive or negative. These observations lead us to discard our previously postulated mechanism in favour of one involving the production of atomic oxygen in the primary photolysis step. The highly variable and negative yields of SO_2 are accounted for by postulating the formation of varying amounts of peroxysulfuric acid in the irradiated droplets.

Keywords: Quantum yield; CO_2; SO_2; Photo-oxidation; CO; Sulfuric acid aerosol

1. Introduction

In a previous paper [1], we reported the observation of CO_2 production during 193 nm ArF laser irradiation of a concentrated sulfuric acid aerosol in the presence of carbon monoxide; it was suggested that this process may play a role in helping to maintain the CO_2 atmosphere of Venus [2]. Our proposed photolysis mechanism is shown below

$$H_2SO_4 + h\nu \longrightarrow HSO_3 + OH \quad (1)$$

$$OH + CO \longrightarrow H + CO_2 \quad (2)$$

$$H + HSO_3 \longrightarrow H_2O + SO_2 \quad (3)$$

where all reactions occur in the liquid phase inside the droplets.

In this paper, we have measured the quantum yields of CO_2 and SO_2 formation for this system and have found that they are of the order of 1% under laboratory conditions, values which may well be sufficient to make them significant in the atmosphere of Venus. We have also found that the above mechanism represents, at the very least, a considerable oversimplification. Although the quantum yield of CO_2 is tolerably reproducible and varies in a sensible manner with variations in the average laser power, CO partial pressure and acid concentration in the droplets, the quantum yield of SO_2 is highly variable and is seldom equal to the CO_2 yield, as the above mechanism would predict. The measured SO_2 yield is commonly larger than the CO_2 yield by a factor of two or more, but is often zero and, in experiments where calibration flows of SO_2 and CO_2 are added to the aerosol flow immediately after irradiation, the yield of SO_2 can be negative. Some probable reasons for this behaviour and a preferred alternative to reactions (1)–(3), involving a primary process which yields atomic oxygen rather than hydroxyl radicals, are given in Section 4.

2. Experimental details

A block diagram of the apparatus is shown in Fig. 1. As in the experiments of Mozurkewich and Calvert [3], the sulfuric acid aerosol was formed by mixing two streams of gas, one of which had been bubbled through fuming sulfuric acid in a thermostat and the other through water in a separate thermostat held slightly below room temperature. The partial pressure of water at the point of mixing was calculated from the gas flow, the vapour pressure of water at the thermostat temperature and the total pressure in the saturator. The partial pressure of SO_3 in its carrier gas (normally argon) immediately prior to the point of mixing was obtained by measuring the absorption of the Hg 253.7 nm line in a 0.42 m absorption cell, using the extinction coefficient measured by Fajans and Goodeve [4]. The final acid concentration in the droplets was calculated iteratively by mass balance, using tabulated vapour pressure data for concentrated sulfuric acid [5]. The size distribution of the droplets was estimated by light scat-

SSDI 1010-6030(95)04176-1

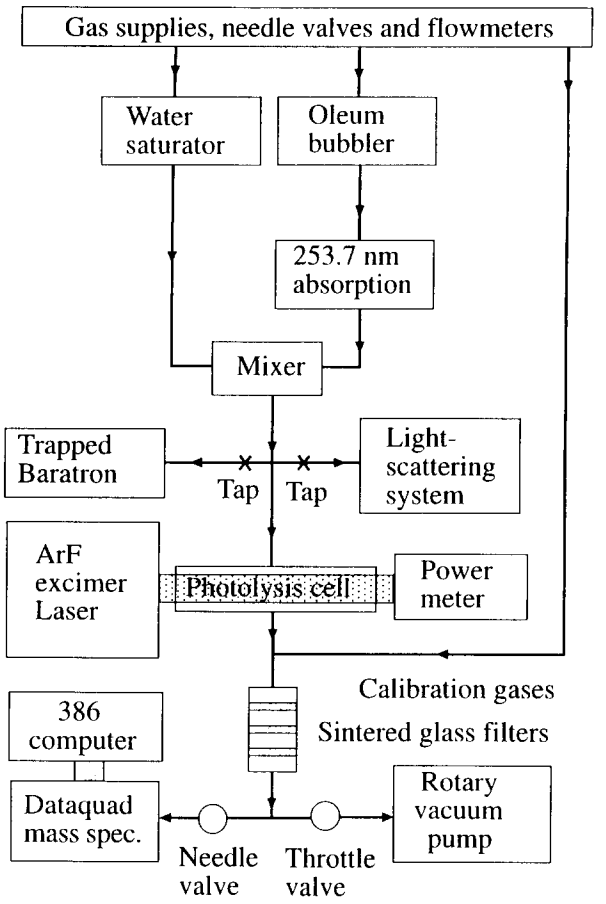

Fig. 1. Block diagram of the aerosol photolysis system. The individual thermostats for the water saturator and oleum bubbler, the optical components and vacuum pump connection for the light scattering system, the light source and detection system associated with the 253.7 nm absorption cell, and most of the taps (glass-key, Teflon-seal, vacuum stopcocks) in the flow lines are not shown.

tering with an He–Ne laser [6,7]. The typical mean diameter was 0.8 μm, with significant scattering at large angles indicating that many smaller particles were present. In the present study no attempt was made to obtain a monodisperse aerosol; nor was any effort made to obtain a reproducible size distribution. This is regarded as a prime topic for future work.

From the mixing point, the stream of gas plus aerosol flowed slowly to the irradiation cell, part of the flow being diverted on occasion to the light scattering cell. The irradiation cell (Fig. 2) was made from an 8 cm length of rectangular cross-section Pyrex tubing with Suprasil end windows. The windows were held in position with halocarbon wax, supported by an external bead of Torr-seal epoxy resin. Small "window cleaning" flows of argon were introduced at each end of the cell but, despite this, the windows gradually became obscured during the course of an experiment by a mist of adherent sulfuric acid droplets. The transmission of the empty cell for 193 nm radiation was determined with a SciTech model 846 power/energy meter. The 193 nm radiation was generated by a Lumonics EX-744 excimer laser, which had its own built-in power meter as part of a system

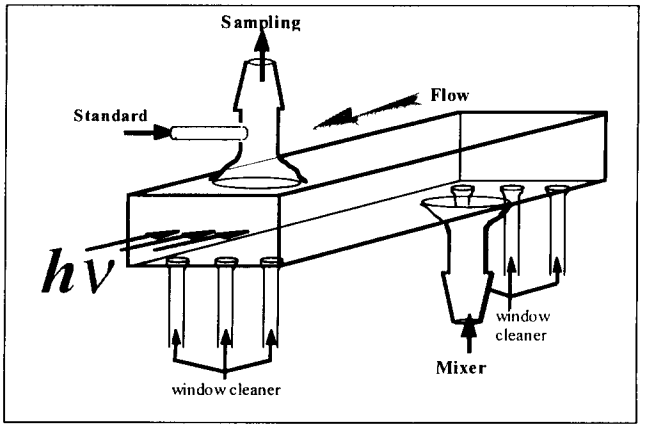

Fig. 2. Diagram of the photolysis cell. Laser light enters from the left; gases enter from lower right. For construction details, see text.

for stabilizing the output power. The readings on the two power meters normally agreed to within 10%. After leaving the irradiation cell, the gas stream flowed through three sintered glass discs, whose function was to remove most of the aerosol droplets, and past a capillary sampling inlet leading via a stainless steel needle valve to a Dataquad model DAQ200 quadrupole mass spectrometer. The mass spectrometer was connected via an RS232 interface to a computer which served both to control the mass spectrometer's operation and to display and store the heights of selected mass peaks as a function of time. In most of the experiments, small calibration flows of CO_2 and SO_2 were introduced into the gas stream immediately after the irradiation cell. The effects of laser irradiation were then observed as changes in the peak heights associated with these calibration flows, measured relative to the peak height at mass 36 (a minor argon isotope which could be measured with the same gain settings as the calibration flows) due to the known flow of argon. After passing the sampling inlet, the gas stream flowed to a rotary vacuum pump via a liquid nitrogen trap. The total pressure in the system (200–600 Torr) was measured with a 0–1000 Torr MKS Baratron, which was protected from contact with the aerosol by a sintered glass filter and a dry-ice/alcohol trap. The measured quantities needed for quantum yield determination were the average laser power during irradiation, the calibration gas flows and the changes in peak heights at masses 64 (SO_2) and 44 (CO_2), relative to the argon internal standard, when the laser was turned on and off. All experiments were carried out at room temperature (approximately 23 °C).

3. Results

A graph of the peak height vs. time is shown in Fig. 3 for one of the better experimental runs in which both quantum yields were positive. Fig. 4 shows a typical run in which the quantum yield of SO_2 was negative. It was not possible to predict in advance whether the yield of SO_2 would be positive

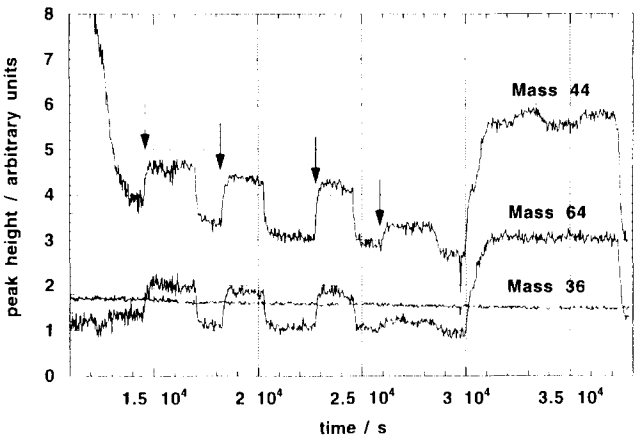

Fig. 3. Time dependence of peak heights during an experiment in which the quantum yields of CO_2 and SO_2 were both positive. Arrows indicate times at which the laser was turned on.

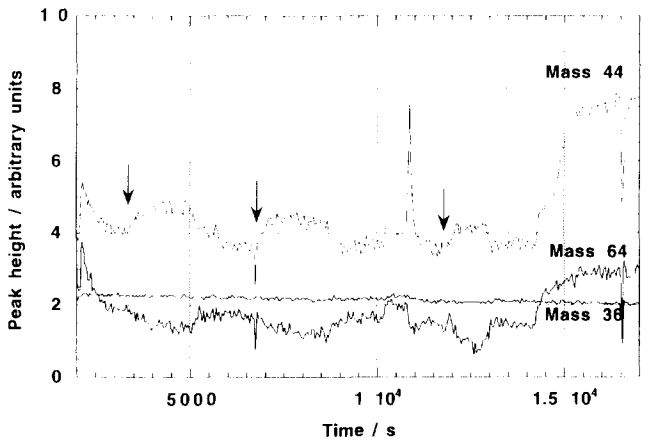

Fig. 4. Time dependence of peak heights during an experiment in which the quantum yield of SO_2 was negative. Arrows indicate times at which the laser was turned on.

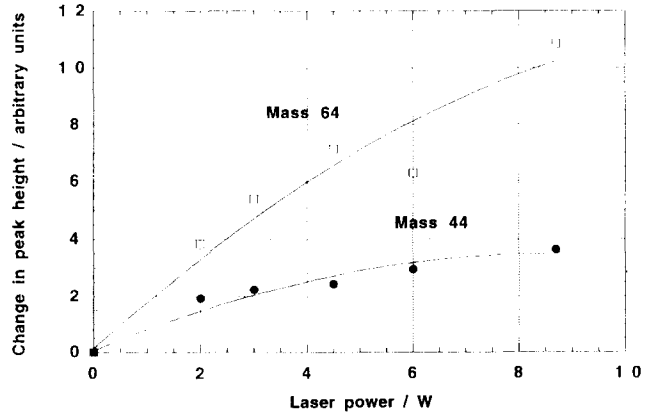

Fig. 5. Variation of the quantum yield with laser power.

or negative. There were also a number of runs carried out with no calibration flow of SO_2 and in which the yield of SO_2 was zero. It seems likely that such runs would also have given a negative SO_2 yield if the calibration flow had been present. The variability of the SO_2 yield may in part be related to uncontrolled variations in the droplet size, a hypothesis which

Table 1
Effect of varying the CO flow on the peak heights at masses 64 and 44

CO flow (sccm)	ΔSO_2	ΔCO_2
22	0.409	0.097
44	0.444	0.221
65	0.288	0.244

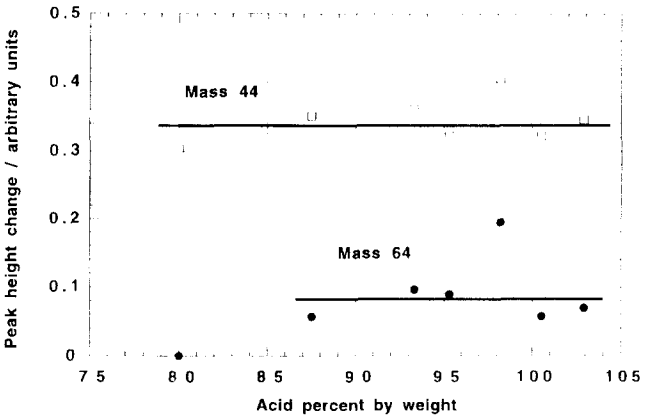

Fig. 6. Variation of the quantum yield with SO_3 flow, expressed in terms of the acid strength in the droplets. Percentages greater than 100 correspond to deficiencies in H_2O.

has still to be tested, and in part to the dissolution of varying amounts of SO_2 in the liquid accumulated on the walls and in the channels of the sintered glass filters, but the observation of negative SO_2 yields clearly requires more drastic adjustment of the mechanism. The addition of a small flow of oxygen before the gas stream entered the irradiation cell had no discernible effect on the CO_2 or SO_2 yield.

In contrast with SO_2, CO_2 always gave a positive quantum yield and the measured CO_2 yield was reasonably constant, although always liable to decrease with time during an experimental run as a consequence of misting of the Suprasil windows. The CO_2 and SO_2 yields showed a tendency towards saturation with increasing laser power (Fig. 5). All quantum yield measurements which contributed to the final average value were made at laser powers well below the onset of saturation. Within the scatter of the results, the CO_2 and SO_2 yields were independent of the CO flow (Table 1) and acid concentration (Fig. 6). The results in Table 1 are not very impressive, but it should be noted that these tests were very difficult to perform because the system took a long time to settle down after any of the gas flows was altered. The range of CO flows used in the experiments was between 50 and 90 standard cubic centimetres per minute (sccm). The mean of 48 measurements of the quantum yield of CO_2 is 0.0119 with a standard deviation of 0.0060. Taking plus or minus twice the standard error of the mean as the 95% confidence limits, we can express this result as 0.012 ± 0.012. Because some of the contributing results will have been affected by misting of the Suprasil windows, this is probably best regarded as a lower limit. No meaning attaches to the average of the measured quantum yields of SO_2.

4. Discussion

Reactions (1)–(3) are sufficient to describe the observations for CO_2 production, but clearly inadequate for SO_2. An alternative mode of CO_2 production would involve the reaction of CO with OH from the photolysis of water, but this can be ruled out because the CO_2 yield is independent of the acid concentration over a range of concentrations (including values for which the partial pressure of gaseous H_2O is negligible) and the molecular absorption coefficient of H_2SO_4 is very large above 190 nm [8], where the absorption by water is weak [9]. We therefore need to consider alternative primary processes and additional secondary processes.

Regarding the primary process (1), this seemed the most plausible choice initially, but there is no independent evidence that this is the only, or even the most important, process. Other possibilities include

$$H_2SO_4 + h\nu \longrightarrow HSO_4 + H \quad (4)$$

and

$$H_2SO_4 + h\nu \longrightarrow H_2SO_3 + O \quad (5)$$

where the HSO_4 from process (4) may possess sufficient internal energy to dissociate into OH and SO_3. This would allow the conversion of CO to CO_2 via reaction (2) and would also, as will be described later, provide a route to an explanation for the negative quantum yields of SO_2. However, this set of reactions does not account for the positive quantum yields of SO_2 observed when the acid strength is well below 100%, i.e. when there could be no SO_2 production by photolysis of SO_3. Thus process (4) can probably be eliminated as a major photodissociation channel.

Process (5) will yield SO_2 and H_2O by the decomposition of H_2SO_3, and will be followed by the direct recombination process

$$CO + O \longrightarrow CO_2 \quad (6)$$

when CO and O are within the same solvent cage. (In the gas phase, process (6) generates significant light emission [10]. It would be interesting to discover whether the emission observed by Lee and coworkers [6] changed its character when CO was added.) Process (5) may also lead to OH production by the secondary reaction

$$H_2SO_4 + O \longrightarrow HSO_4 + OH \quad (7)$$

On the basis of the available thermochemical data [11,12], reaction (7) is approximately thermoneutral in the gas phase and may be fast enough to be diffusion limited in the liquid phase.

The production of OH is required for one of two possible explanations of the negative quantum yields of SO_2 that are often observed when the SO_2 calibration standard is introduced after the photolysis cell. This explanation begins with the formation of H_2O_2 by

$$OH + OH \longrightarrow H_2O_2 \quad (8)$$

a reaction which is known to occur in the liquid cage during the radiolysis of water [13], and will be followed by

$$H_2O_2 + SO_2 \longrightarrow H_2SO_4 \quad (9)$$

The H_2O_2 produced during irradiation will survive to oxidize SO_2 that is introduced later. A telling point against this mechanism is that it involves OH radicals from two separate primary photolysis events, so that the negative SO_2 yield should be dependent on the square of the laser power, or should at least show a much more positive dependence on the laser power than the CO_2 yield; our results provide no support for this conclusion. When the laser power is varied, the negative yields of SO_2 behave in a similar manner to the positive yields of SO_2 and CO_2, i.e. the magnitude of the quantum yield tends to fall off at high laser power.

An alternative mechanism, which is now favoured, involves process (7) leading to peroxysulfuric acid rather than $OH + HSO_4$, where the peroxysulfuric acid will survive to remove the SO_2 introduced later. The direct insertion reaction of O with H_2SO_4 to form H_2SO_5 is likely to be slow, but the peroxysulfuric acid may be formed in two steps, reaction (7) being followed by the association

$$HSO_4 + OH \longrightarrow H_2SO_5 \quad (10)$$

within the same liquid cage. At present our results favour primary process (5), followed by reactions (6), (7) and (10), but further work is needed before this conclusion can be regarded as definite. Theoretical studies of the transition responsible for the H_2SO_4 photodissociation at 193 nm, and experimental measurements of the OH quantum yield from this process, are highly desirable.

Detailed model calculations are needed to show what role, if any, the photo-oxidation of CO to CO_2 in the sulfuric acid aerosol may play in the atmosphere of Venus. In view of the vast extent of sulfuric acid clouds of Venus, a quantum yield of the order of 1% may well be large enough for the process to be significant.

Acknowledgements

We are grateful to A. Fried for helpful discussions. This research was supported by the University of Canterbury Research Committee and by grant 94-UOC-36-181 from the New Zealand Foundation for Research, Science and Technology.

References

[1] C.T. Mills and L.F. Phillips, *J. Photochem. Photobiol. A: Chem., 74* (1993) 7.
[2] V.A. Krasnopolsky, *Photochemistry of the Atmospheres of Mars and Venus*, Springer-Verlag, Berlin, 1986.
[3] M. Mozurkewich and J.G. Calvert, *J. Geophys. Res., 93* (1988) 15 889.
[4] E. Fajans and C.F. Goodeve, *Trans. Faraday Soc., 32* (1936) 511.

[5] J.I. Gmitro and J. Vermeulen, *Am. Inst. Chem. Eng. J., 10* (1964) 740.
[6] Y.G. Jin, H.C. Zhou, M. Suto and L.C. Lee, *J. Photochem. Photobiol. A: Chem., 52* (1990) 225.
[7] J. Westergren, Determination of size distribution of spherical sulfuric acid aerosols by light scattering, *M.Sc. Thesis*, Chalmers University of Technology, Göteborg, 1994.
[8] J.L.R. Morgan and R.H. Crist, *J. Am. Chem. Soc., 49* (1927) 338.
[9] D.R. Lide (ed.), *Handbook of Chemistry and Physics*, CRC Press, Boston, 71st edn., 1991, pp. 9–138; see also R.D. Hudson, *Rev. Geophys. Space Phys., 9* (1971) 305.
[10] B.H. Mahan and R.B. Solo, *J. Chem. Phys., 37* (1962) 2669.
[11] S.G. Lias, J.E. Bartmess, J.F. Liebman, J.L. Holmes, R.D. Levin and W.G. Mallard, *J. Phys. Chem. Ref. Data, 17* (Suppl. 1) (1988).
[12] W.B. DeMore, S.P. Sander, D.M. Golden, R.F. Hampson, M.J. Kurylo, C.J. Howard, A.R. Ravishankara, C.E. Kolb and M.J. Molina, *Chemical Kinetic and Photochemical Data for Use in Stratospheric Modeling*, Evaluation Number 11, Jet Propulsion Laboratory, Pasadena, 1994.
[13] J.W.T. Spinks and R.J. Woods, *An Introduction to Radiation Chemistry*, Wiley, New York, 1964.